

# Loss of genomic methylation causes p53-dependent apoptosis and epigenetic deregulation

Laurie Jackson-Grusby<sup>1</sup>, Caroline Beard<sup>1</sup>, Richard Possemato<sup>1,2</sup>, Matthew Tudor<sup>1,2</sup>, Douglas Fambrough<sup>1</sup>, Györgyi Csankovszki<sup>1,2</sup>, Jessica Dausman<sup>1</sup>, Peggy Lee<sup>3</sup>, Christopher Wilson<sup>3</sup>, Eric Lander<sup>1,2</sup> & Rudolf Jaenisch<sup>1,2</sup>

Cytosine methylation of mammalian DNA is essential for the proper epigenetic regulation of gene expression and maintenance of genomic integrity. To define the mechanism through which demethylated cells die, and to establish a paradigm for identifying genes regulated by DNA methylation, we have generated mice with a conditional allele for the maintenance DNA methyltransferase gene *Dnmt1*. Cre-mediated deletion of *Dnmt1* causes demethylation of cultured fibroblasts and a uniform p53-dependent cell death. Mutational inactivation of *Trp53* partially rescues the demethylated fibroblasts for up to five population doublings in culture. Oligonucleotide microarray analysis showed that up to 10% of genes are aberrantly expressed in demethylated fibroblasts. Our results demonstrate that loss of *Dnmt1* causes cell-type-specific changes in gene expression that impinge on several pathways, including expression of imprinted genes, cell-cycle control, growth factor/receptor signal transduction and mobilization of retroelements.

## Introduction

Epigenetic gene regulation is important in determining cellular fates during development and is accomplished through the modulation of chromatin packaging<sup>1</sup>. Cytosine methylation is thought to establish the compact and silenced chromatin state in vertebrate genomes through binding methyl-DNA binding proteins and recruitment of histone deacetylases<sup>2</sup>. This process is linked to cellular differentiation and developmental potential such that totipotent embryonic cells from blastocysts or primordial germ cells represent the most undermethylated cell types, whereas somatic cells show elevated methylation levels as tissue-specific patterns of methylation are acquired during differentiation<sup>3</sup>. Thus, it has been speculated that heritable DNA methylation states may serve to regulate cell-type-specific gene expression and, by extension, cellular differentiation.

Three genes are required to establish and maintain genomic methylation: those encoding the *de novo* methyltransferases *Dnmt3a* and *Dnmt3b* and the maintenance enzyme *Dnmt1*. Mutational analysis in mice has shown that they are all essential genes, with the earliest lethality seen shortly after gastrulation in *Dnmt1*-null embryos<sup>4–6</sup>. Aberrant regulation of several imprinted genes<sup>7</sup> and the gene *Xist* (refs. 8,9) has been observed in *Dnmt1*-deficient embryos. Moreover, depletion of *Dnmt1* from *Xenopus laevis* embryos also causes embryonic lethality and inappropriate gene expression<sup>10</sup>. These data are consistent with the notion that DNA methylation is required for transcriptional silencing during mammalian development.

Aberrant hypermethylation also causes transcriptional silencing of tumor-suppressor genes in human tumors, which has led to the proposal that DNA methyltransferases might be good targets for anti-cancer pharmaceuticals<sup>11,12</sup>. Inhibition of *Dnmt1* can prevent

intestinal polyp formation in *Apc<sup>Min</sup>* mice<sup>13</sup>; however, tumors with genes silenced by hypermethylation also show widespread genomic hypomethylation, which may contribute to chromosome instability<sup>14</sup> and tumor progression. Mutations in human *DNMT3B* have been shown to cause centromeric instability-facial anomalies syndrome (ICF syndrome, MIM 242860), which is characterized by loss of pericentromeric repeat methylation and an associated chromosomal instability<sup>6,15,16</sup>. Therefore, a more thorough description of the transcriptional changes in cells with altered DNA methylation levels is required to understand the paradoxical risks and benefits of induced DNA hypomethylation.

The usefulness of the constitutional *Dnmt1* mutants for studying the cellular response to demethylation has been limited by the early lethality and the stochastic cell death observed throughout the mutant embryos<sup>5,9</sup>. It is likely that multiple genetic pathways become deregulated in response to demethylation and some may be cell-type specific. Therefore, we have used the Cre-*loxP* system<sup>17</sup> to conditionally inactivate *Dnmt1*, and studied the effects of demethylation in homogeneous cultures of primary mouse embryonic fibroblasts. Here we show that loss of *Dnmt1* from somatic cells causes p53-dependent apoptosis and global induction of gene expression.

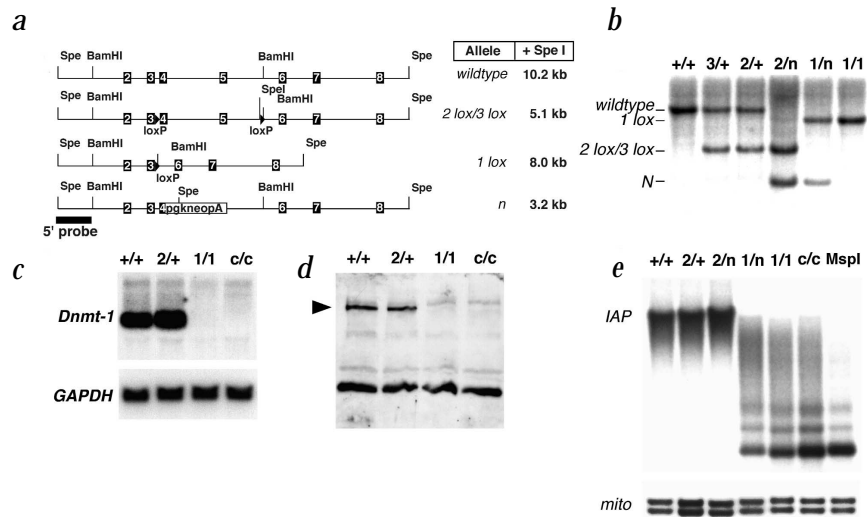
## Results

### Characterization of the conditional *Dnmt1* allele

We created a conditional mutation in the mouse gene *Dnmt1* by inserting *loxP* sites flanking exons 4 and 5 (*Dnmt1<sup>tm4Jae</sup>*, hereafter referred to as *Dnmt1<sup>2lox</sup>*; Fig. 1a) in embryonic stem (ES) cells. Cre-mediated deletion of these exons (*Dnmt1<sup>1lox</sup>*; Fig. 1b) causes an out-of-frame splice from exon 3 to exon 6 and produces an RNA encoding the first 67 of 1,619 amino acids, lacking the motifs

<sup>1</sup>Whitehead Institute for Biomedical Research, and <sup>2</sup>Biology Department, Massachusetts Institute of Technology, Cambridge, Massachusetts, USA. <sup>3</sup>Departments of Immunology and Pediatrics, University of Washington, Seattle, Washington, USA. Correspondence should be addressed to R.J. (e-mail: jaenisch@wi.mit.edu).

**Fig. 1** Conditional inactivation of mouse *Dnmt1* in ES cells. **a**, Schematic of the constructed alleles. Note that the *Dnmt1*<sup>3lox</sup> allele is an intermediate to the final *Dnmt1*<sup>2lox</sup> allele, in which the floxed selection cassette (not diagrammed) is present in the downstream *Bam*HI site. Fragment lengths for the diagnostic *Spe*I digest are indicated. **b**, Genotyping Southern blot shows the altered structure of the *Dnmt1* locus. *Dnmt1* genotypes are indicated above each lane, and the position of the *Spe*I fragments for each allele are labeled. The *Dnmt*<sup>fl</sup> and *Dnmt*<sup>c</sup> alleles have been characterized<sup>4,5</sup>. **c**, Northern blot of RNA from ES cells probed with a 2-kb *Dnmt1* cDNA fragment corresponding to the catalytic domain. The blot was reprobbed with *Gapdh* to demonstrate equal loading. *Dnmt1* genotypes are indicated above each lane. **d**, Western blots of ES cell extracts probed with a C-terminal antibody probe. *Dnmt1* is indicated with an arrowhead. The non-specific crosshybridizing proteins serve as internal loading standards. *Dnmt1* genotypes are indicated above each lane. **e**, Southern blots of *Hpa*II-digested genomic DNA probed with IAP or with a mitochondrial sequence as a digestion and loading control. *Dnmt1* genotypes are indicated above each lane.



for localization and the entire catalytic domain of the protein<sup>18</sup>. To confirm the functional status of the *Dnmt1*<sup>2lox</sup> and *Dnmt1*<sup>1lox</sup> alleles, we assessed the activities of both the presumed silent mutation in the *Dnmt1*<sup>2lox</sup> allele and the mutant *Dnmt1*<sup>1lox</sup> allele by northern- and western-blot analyses in ES cells (Fig. 1c,d). Comparison of the *Dnmt1*<sup>2lox/+</sup> cells with wild-type J1 cells showed indistinguishable *Dnmt1* RNA and *Dnmt1* protein levels, consistent with the presumption that the *loxP* insertions were silent mutations. *Dnmt1*<sup>1lox/1lox</sup> ES cells also appeared identical to the previously characterized null *Dnmt1*<sup>c/c</sup> ES cells<sup>4</sup> (*Dnmt1*<sup>tm1Lj</sup>). Finally, the normally highly methylated intracisternal A particle sequences (IAP, Fig. 1e), centromeric satellite (data not shown) and Moloney murine leukemia virus (data not shown) all had fully methylated DNA in cell lines with a *Dnmt1*<sup>2lox</sup> allele and extensive demethylation in *Dnmt1*<sup>1lox/1lox</sup> and *Dnmt1*<sup>c/c</sup> cells.

#### Somatic-cell inactivation of *Dnmt1* causes demethylation and p53-dependent apoptosis

To establish somatic cell cultures for conditional inactivation of *Dnmt1*, we generated a mouse strain carrying the conditional *Dnmt1*<sup>2lox</sup> allele by injection of *Dnmt1*<sup>2lox/+</sup> cells into mouse blastocysts. *Dnmt1*<sup>2lox/2lox</sup> mice are viable and fertile with normal levels of somatic methylation in all tissues examined (data not shown). We have chosen primary embryonic fibroblasts derived from these mice as a model cell type to study the effects of demethylation because these cultures are easily obtained and fairly homogeneous. Cre-mediated recombination was carried out *in vitro* by infection of primary fibroblast cultures with high-titer retroviral supernatants. We subcloned the *cre* gene into the retroviral vector pMX-puro (pMXCP; Fig. 2a; ref. 19) to allow selection of retrovirally infected cells with puromycin. The methylation status of *Dnmt1*<sup>2lox/2lox</sup> fibroblasts infected with pMXCP or the parental pMXpuro vectors is shown (Fig. 2b). Notably, Cre-expressing fibroblasts show progressive demethylation from three to five days postinfection that is comparable to that seen in *Dnmt1*<sup>1lox/1lox</sup> ES cells. Therefore, conditional inactivation of *Dnmt1* with this allele provides a population of cells to study the consequences of demethylation.

Genomic demethylation in primary fibroblasts causes a uniform, cell-lethal phenotype between five and six days postinfection with Cre (Fig. 3). This is in contrast to the phenotype of

*Dnmt1*-deficient ES cells, which proliferate normally in culture unless they are induced to differentiate. Cells from both postgastrulation *Dnmt1*-mutant embryos and differentiating cultures of *Dnmt1*-mutant ES cells show stochastic apoptotic cell death<sup>5,9</sup>. TUNEL assays performed on *Dnmt1*<sup>1lox/1lox</sup> primary fibroblast cultures at 5.5 and 6 days post-infection with Cre showed approximately 20% of cells undergoing apoptosis at each time point (Fig. 3b). To quantify the proliferative capacity of methylation-deficient cells, we serially passaged and counted viable cells every three days. *Dnmt1*<sup>1lox/1lox</sup> primary cultures showed extensive cell death and failed to show a quantifiable number of cell divisions, whereas control *Dnmt1*<sup>2lox/2lox</sup> cultures carried out four population doublings (Fig. 3c).

The widespread apoptotic phenotype of these *Dnmt1*-deficient fibroblasts suggested that DNA demethylation might represent an endogenous signal of DNA damage. We considered that inactivation of the *Trp53* tumor-suppressor gene might rescue this cell lethal phenotype, as *Trp53* is activated in response to a wide variety of signals of DNA damage<sup>20</sup>. Additionally, other embryonic lethal mutations, such as those in *Rad51*, *Brca1* and *Brca2*,

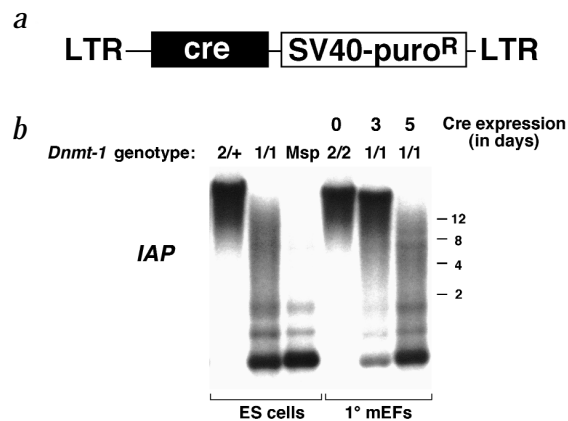
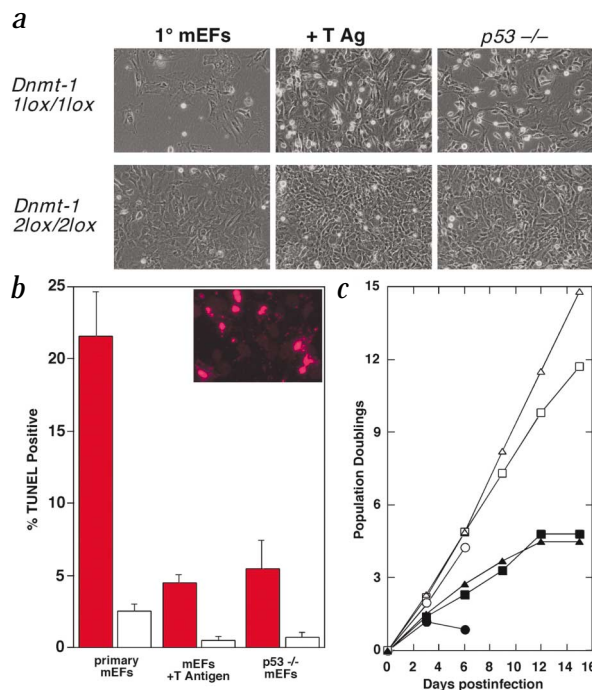


**Fig. 2** Conditional inactivation of mouse *Dnmt1* in embryonic fibroblasts. **a**, Schematic of the *cre* retroviral vector. **b**, Southern blots of *Hpa*II-digested genomic DNAs probed with an IAP probe.



which are involved in maintaining genomic integrity, have been shown to be partially rescued by *Trp53* mutations<sup>21–23</sup>. We transformed *Dnmt1*<sup>2lox/2lox</sup> fibroblast cultures with retrovirally transduced SV40 large T antigen to inactivate p53. In addition, a *Trp53* deletion allele<sup>24</sup> was bred into the *Dnmt1*<sup>2lox/2lox</sup> mouse colony and used to derive *Trp53 Dnmt1* double-mutant fibroblast cultures. In contrast to the *Trp53* wild-type cultures, both the T-antigen-transformed cells and the *Trp53*-mutant cells survived Cre-mediated deletion of *Dnmt1* beyond six days post-infection (Fig. 3a). TUNEL analysis showed fourfold fewer apoptotic cells (5.4% versus 22%) in the *Dnmt1*<sup>1lox/1lox</sup> *Trp53*-deficient cultures compared with the *Trp53* wild-type cultures, indicating that demethylation-induced cell death is mediated in part by p53. A substantial percentage of both T-antigen-transformed and *Trp53*-mutant cultures were TUNEL positive following inactivation of *Dnmt1*, suggesting the involvement of additional pathways that cause cell death in these cultures (Fig. 3b).

To show that the p53 rescue from demethylation-induced cell death was not simply caused by an inhibition of Cre, we determined recombination at *Dnmt1* by Southern-blot analysis with quantitation by phosphoimaging (Fig. 4a). Extensive Cre-mediated recom-

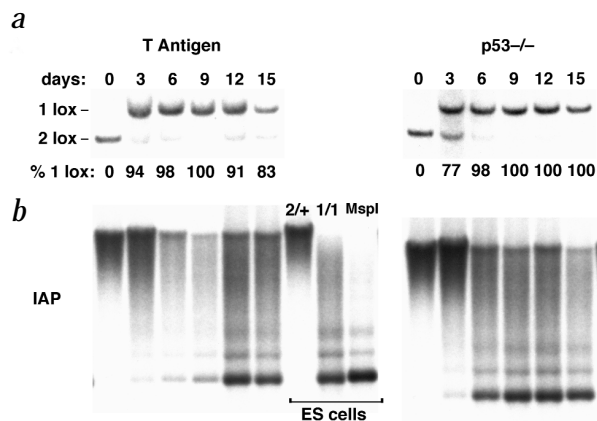


**Fig. 3** p53-dependent apoptosis and growth arrest of *Dnmt1*-deficient fibroblasts. **a**, Phase-contrast views of mutant *Dnmt1*<sup>1lox/1lox</sup> and control *Dnmt1*<sup>2lox/2lox</sup> fibroblasts transduced with pMXCP or pMXpuro, respectively. We plated 10<sup>6</sup> cells at 3 d post infection, and changed the medium after 2 d to remove puromycin-sensitive cells. Photos were taken 24 hours after the media change. Note the extensive cell loss in the primary *Dnmt1*<sup>1lox/1lox</sup> mEFs (top left) compared with the cells rescued by T-antigen expression (middle) or by mutational inactivation of *Trp53* (top right). **b**, TUNEL staining was performed at 5.5 and 6 days postinfection with pMXCP (filled bars) or pMXpuro (open bars). Data are presented as averaged counts for three cultures with both time points included. An example of TUNEL-positive primary *Dnmt1*<sup>1lox/1lox</sup> fibroblasts is shown in the inset. **c**, Population doublings of mutant *Dnmt1*<sup>1lox/1lox</sup> (filled symbols) and control *Dnmt1*<sup>2lox/2lox</sup> (open symbols) fibroblast cultures. We plated 10<sup>6</sup> cells in 10-cm dishes and counted total cell numbers after 3 d. Cells were serially passaged according to this protocol until no further division was observed. Circle, primary mEFs; triangle, transformed mEFs; square, *Trp53*<sup>-/-</sup> mEFs.

ination at *Dnmt1* was seen by three days postinfection in both T-antigen-transformed and *Trp53*-mutant fibroblasts. From day 6 through day 9 postinfection, the T-antigen-transformed cells were uniformly recombined, but we saw a minor population of unrecombined *Dnmt1*<sup>2lox/2lox</sup>-transformed cells that increased in abundance at later time points. Selection of pMXCP-infected cultures with a fivefold higher concentration of puromycin did not eliminate the contaminating *Dnmt1*<sup>2lox/2lox</sup>-transformed cells (data not shown), indicating that these cells failed to express *cre*. This observation is consistent with studies<sup>25</sup> showing stochastic silencing of the 5' gene of a similarly constructed retroviral vector. Nevertheless, pure populations of *Trp53 Dnmt1* double-mutant cells are reproducibly generated from 6 to 15 days postinfection with this approach (Fig. 4a).

To assess genomic methylation in these fibroblast cultures, we analyzed the methylation level of repetitive sequences. Southern-blot analysis using an IAP probe demonstrated that both the *Trp53 Dnmt1* double-mutant fibroblast cultures and the T-antigen-transformed *Dnmt1*<sup>1lox/1lox</sup> fibroblasts were extensively hypomethylated (Fig. 4b). Residual methylation was seen at all time points examined, whereas IAP elements were completely demethylated in both the primary *Dnmt1*<sup>1lox/1lox</sup> fibroblasts and ES cells. Similar levels of demethylation were observed at centromeric  $\alpha$ -satellite sequences in each of the *Dnmt1*<sup>1lox/1lox</sup> cells, including the ES cells and the *Trp53*-mutant or T-antigen-transformed fibroblasts (data not shown). Thus, these *Dnmt1*<sup>1lox/1lox</sup> cultures serve as a useful model system to study the molecular and cellular consequences of demethylation.

#### Reduced proliferation in *Dnmt1*-mutant fibroblasts

To quantify the proliferative capacity of the *Dnmt1*-deficient cultures, we made serial passages and calculated population doublings over time (Fig. 3c). Both the *Trp53*-mutant and T-antigen-transformed *Dnmt1*<sup>1lox/1lox</sup> cultures went through approximately five doublings over the course of two weeks in culture. This indicates that expression of *Dnmt1* is not an absolute requirement during DNA replication despite its localization to replication foci<sup>26</sup> and interaction with proliferating cell nuclear antigen<sup>27</sup> (PCNA). The control *Dnmt1*<sup>2lox/2lox</sup> cultures, however, doubled at almost three times the rate of the demethylated cells (1 division/day versus 1 division/3 days, respectively). Moreover, there was an absence of proliferation between day 12 and 15 from the *Trp53*-deficient *Dnmt1*<sup>1lox/1lox</sup> cultures, consistent with the possibility that epigenetic deregulation may lead to cell-cycle arrest.

**Fig. 4** Recombination and DNA methylation status of *Dnmt1*, *Trp53* double-mutant cultures. **a**, Cre-mediated recombination at *Dnmt1* analyzed by Southern blot. T-antigen-transformed cells are on the left, *Trp53*<sup>-/-</sup> cells are on the right. Blots were exposed to a Fuji phosphoimaging plate which was used to determine percentage recombination. **b**, DNA methylation levels assayed by Southern blots of *HpaII*-digested genomic DNA hybridized with an IAP probe.

**Table 1 • GeneCHIP analysis of altered gene expression caused by demethylation**

	no. of sample pairs	minimum no of "P" calls	no. of expressed genes	Genes up > 2-fold no. (%)	Genes down >2-fold no. (%)
T antigen lines	4	3	5623	27 (0.48%)	39 (0.69%)
<i>Trp53</i> <sup>-/-</sup> 1° mEFs	4	3	5717	562 (9.8%)	48 (0.83%)
Total	8	4	5996	268 (4.5%)	105 (1.8%)

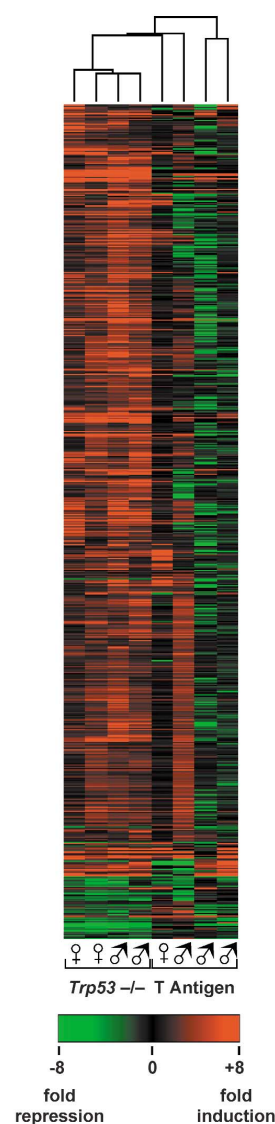
The number of measurable genes were determined by counting present (P) calls for each gene in the data set. Significant differences in expression between *Dnmt1* mutant and wild-type cells were observed with the indicated number of P calls for each data set. Numbers of increased and decreased genes include the entries with 2-fold or greater change in expression ( $P \leq 0.05$ , Student's *t*-test).

### Oligonucleotide arrays show global increases in gene expression in *Dnmt1*-mutant fibroblasts

We used transcriptional profiling using oligonucleotide arrays<sup>28</sup> to assess global changes in gene expression caused by demethylation. Targets were prepared from *Dnmt1*<sup>2lox/2lox</sup> and *Dnmt1*<sup>1lox/1lox</sup> cellular RNA isolated six days after retroviral infection when Cre-mediated recombination and demethylation were complete (Fig. 4). We chose this early time point to focus on expression changes that may be directly caused by demethylation rather than secondary expression changes, which may occur later in the cultures. We analyzed eight pairs of targets derived from four independent T-antigen-transformed fibroblast cell lines and primary fibroblasts from four individual *Trp53*-mutant embryos. Of the 13,103 total feature sets present on the Affymetrix GeneCHIP arrays, 5,996 showed significant expression in at least 4 of 16 samples. Statistical analysis (paired *t*-test) identified only 66 genes (1.2%) with significant expression differences ( $P \leq 0.05$ ) of twofold or greater among the four transformed cell lines following demethylation. A similar comparison of the p53-deficient primary cells identified 610 genes (10.7%) with deregulated expression (Table 1). Analysis of all 8 mutant average difference values compared with the 8 control values identified 373 altered genes (6.2%). It has been hypothesized that DNA methylation may serve to silence spurious transcription<sup>29</sup>. In support of this hypothesis, our data indicate that at least 4–10% of detectable genes are induced twofold or greater by demethylation (Table 1 and Fig. 5). In contrast, only 1–2% of detectable genes were downregulated. This suggests that global hyperactive gene expression may be a phenotype of *Dnmt1*-deficient cells.

To ensure that scaling of the data did not introduce bias, we examined expression of *Gapdh* and ribosomal protein genes *rpl8*, *rpl12* and *rpl18* as controls. Average difference values were used to calculate the relative expression for each of the control genes in the primary fibroblasts and in the cell lines (*Gapdh* ratio of *Dnmt1* mutant/wild type was  $1.08 \pm 0.12$  and  $1.08 \pm 0.19$ , respectively, and ribosomal protein genes showed ratios of  $0.98 \pm 0.18$  and  $0.95 \pm 0.20$ , respectively;  $n=6$  feature sets per gene). That these ratios are close to 1.0 supports the linear regression fit for the data set.

**Fig. 5** Transcriptional profiling of gene expression changes in *Dnmt1*-mutant fibroblasts. Two-dimensional hierarchical clustering of eight sample pairs and 1204 genes, selected as significantly changed by a paired Student's *t*-test ( $P \leq 0.05$ ), was performed on log-transformed fold-change data using average linkage clustering with uncentered correlation<sup>52</sup>. The profiles demonstrate the reproducible hyper-expression phenotype of the *Dnmt1*-*Trp53* double-mutant fibroblasts.



Further biological validation of the data can be gleaned by examining the individual genes deregulated in *Dnmt1*-deficient fibroblasts. As predicted, *Dnmt1* expression in mutant cells was reduced to less than 5% of that seen in wild type (Table 2). Deregulation of several imprinted genes (*Tdag*, *Xist*, *H19*, *Igf2*, *Grb10*, *Peg3*) and repetitive sequences (IAP, L1, G7e) previously known to be regulated by methylation were identified in these comparisons (Table 2), which provides further biological validation of the list of altered genes. Although oligonucleotide arrays may not be sensitive detectors for low-level transcriptional noise, the genes detected here support the emerging view that DNA methylation is in fact an essential mechanism for genome-wide transcriptional regulation.

Among the list of over 600 genes found with altered expression, approximately half represent uncharacterized EST clones. The deregulated named genes encode chromatin and silencing factors, transcription factors, DNA-repair proteins, tumor suppressors and oncogenes, interferon and other signaling pathway components, and cytoplasmic and nuclear enzymes. We also saw an induction of MHC genes and a downregulation of collagen genes. Eleven tissue-specific genes, including placental lactogen I, endoglin and the testis-specific genes *Dazl* and *Tcte3*, were ectopically expressed in *Dnmt1*-mutant fibroblasts.

**Table 2 • Genes induced or repressed by genomic demethylation in fibroblast cultures**

Gene	Accession Number	Fold $\Delta$	Description	Gene	Accession Number	Fold $\Delta$	Description
<b>Methylation</b>				<b>Apoptosis/Stress response</b>			
Ahcy	L32836	3.0	SAH hydrolase	Hif1a	X95580	3.9	hypoxia inducible factor
Dnmt1	X14805	-39	DNA methyltransferase	Traf3	U33840	3.7	Tnf receptor-associated
<b>Imprinted</b>				Hsp25	I07577	3.2	heat shock protein
Tdag	U44088	4.4	TDAG51	Hsp105	D67016	2.7	heat shock protein
Xist	L04961	3.5	Xist	Traf4	X92346	2.5	Tnf receptor-associated

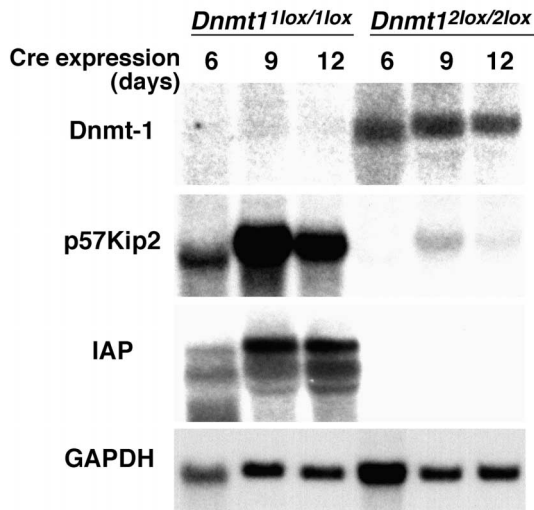
continued on next page



Table 2 • (continued)

Gene	Accession Number	Fold Δ	Description	Gene	Accession Number	Fold Δ	Description
Peg3	U48804	-2.4	Zn-finger protein Pw1 gene	Adprp1	aa119245	2.4	pADP-ribose polymerase
Grb10	U18996	-3.1	growth factor receptor-b.p.	Bag1	AF022223	2.1	bcl-2 binding protein
Igf2	U71085	-4.5	insulin-like growth factor 2	<b>Cell cycle</b>			
H19	X58196	-8.9	H19	Cdkn1a	U09507	3.7	cyclin kinase inhibitor
<b>Retroviral/Repetitive elements</b>				Chek1	AF016583	3.5	checkpoint kinase
IAP	C78676	47.4	intracisternal A particle	Rpa2	D00812	3	Rad51 homolog
G7e	U69488	4.6	viral envelope protein	Ccng2	af005885	2.6	cyclin G2
L1Md-Tf14	D84391	3.1	L1 repeat	Cdc25a	U27323	2.5	cell division cycle 25A
IAP	AF003867	-2.3	intracisternal A particle	Gas2	M21828	-3	growth arrest specific
<b>Chromatin/silencing</b>				Cks1	AA032836	-4.4	cyclin kinase regulation
Slbp	U75680	3.7	histone stem-loop b. p.	<b>Tumor Suppressor/oncogene</b>			
Hmgi	J04179	2.4	nonhistone HMG protein	Junb	U20735	13.4	Jun-B oncogene
Sin3a	u22394	2.4	SIN3 yeast homolog A	Ect2	L11316	4.1	Ect2 oncogene
Tif1b	U67303	2.3	TIF1B	Csk	U05247	2.6	c-Src kinase
Cenpa	AA060808	-2.0	centromere autoantigen A	Catnb	M90364	2.3	b-Catenin
Hmg1	Z11997	-2.1	HMG protein 1	Dp1	U28168	2	adenomatosis polyposis coli
<b>DNA recombination/Repair</b>				Rela	M61909	2	v-rel oncogene homolog A
Tdg	aa407018	3.9	Thymine-DNA glycosylase	tsg101	U52945	2	tumor susceptibility gene
Rad52	U06837	2.3	RAD52 homolog	Nmyc1	M29211	-25.1	Nmyc1
Mre11a	U58987	2.2	putative endo/exonuclease	<b>Growth Factor/receptor/signaling</b>			
Pold1	Z21848	-3.8	DNA polymerase delta 1	Gro1	J04596	77	GRO1 oncogene
<b>Transcription factor</b>				Scya2	M19681	26.4	small inducible cytokine
Pea3	X63190	10.3	polyoma enhancer activator	Ereg	D30782	11.1	epiregulin
Nfe2l2	U70475	4.8	erythroid nuclear factor2	Jak2	L16956	6.4	janus kinase 2
Zfp147	D63902	4.1	zinc finger protein	Sema3c	X85994	5.2	semaphorin E
Zfp36	M58691	3.8	zinc finger protein	Pdgfa	M29464	5.2	PDGFA
Klf4	U20344	3.3	gut, Kruppel-like factor	Sfrp1	U88566	4.4	frizzled related
Zfp64	U49046	3.1	zinc finger protein	Cmkor1	AF000236	4.3	Chemokine orphan receptor
Gata2	AB000096	2.7	GATA2	Cish3	U88328	3.9	SOCS-3
Cebpa-rs1	U19891	2.1	C/EBP, related sequence 1	Epha2	U07634	3.3	Eph receptor A2
Crabp1	X51715	-11.7	cellular retinoic acid-b. p.	Gpcr12	D21061	3.2	G-protein coupled receptor
<b>IFN pathway</b>				Csf1	M21952	3	M-CSF
Ifi202a	M31418	6.3	interferon activated gene	Il10rb	U53696	3	IL10 receptor beta
Scyb10	M33266	6.0	interferon activated gene	Rgs16	U94828	2.8	regulator of G proteins
Ifi203	af022371	5.8	interferon activated gene	Thbs2	I07803	2.6	thrombospondin 2
Ifit1	aa616578	5.7	interferon activated gene	Map2k3	D87115	2.5	MAP kinase kinase 3b
Irf7	U73037	4.7	interferon regulatory factor	Bin1	U86405	2.4	brain amphiphysin 2
Mx2	J03368	4.5	myxovirus resistance 2	Fgfr1	M33760	2.3	FGFR1
Isg15	X56602	3.2	interferon activated gene	Il1rap	X85999	2.1	IL-1 receptor accessory
Eif2ak2	M65029	3.1	ds RNA dep. protein kinase	Efnb1	Z48781	-2	ephrin B1
Ifit3	I32974	3.0	interferon activated gene	Ldlr	X64414	-2.2	LDL receptor
Ifngr	J05265	2.2	Interferon g-receptor	Fzd8	U43321	-3.7	frizzled 8
<b>MHC</b>				<b>Insulin-like growth factor pathway</b>			
LOC56628	M69070	24.8	MHC class I antigen	Igfbp6	X81584	2.6	Igf binding protein 6
H2-T10	M35244	8.5	Histocompatibility 2	Cyr61	M32490	2.5	Igf binding protein 10
H2-T23	M11284	5	Histocompatibility 2	<b>Collagens</b>			
H2-D	M69068	4.6	Histocompatibility 2	Col6a2	X65582	-2	procollagen VI, a-2
H2-Q7	M29881	3.8	Histocompatibility 2	Col5a1	aa030649	-2.1	collagen a1(V)
H2-K	U47329	3.8	Histocompatibility 2	Col1a1	D38162	-2.2	procollagen XI, a-1
H2-M3	U18797	2.4	MHC class I antigen	Col6a1	X66405	-2.6	procollagen VI, a-1
<b>Tissue Specific</b>				Col9a1	M32136	-12.2	a-1 typeIX collagen
Slpi	U73004	35.7	leukoprotease inhibitor	<b>Other</b>			
Pem	M32484	14.5	placental homeobox	Ttgn2	D50032	3.6	TGN38A
Eng	X77952	6.9	endoglin	Gtf2h1	AJ002366	2.8	TFIIH, 62 kD subunit
Ptgs2	M64291	6.1	prostaglandin synthase 2	Eif3	U14172	2.8	translation initiation factor
Dazl	X95724	5.8	DAZ-like autosomal	Rpo2-1	U37500	2.6	RNA polymerase II 1
Xlr3b	L22977	4.5	B-cell surface antigen 3b	Tk1	M19438	2.5	thymidine kinase 1
Procr	I39017	4.2	endothelial receptor	Cyp2e1	L11650	2	cytochrome P450
Pl1	M35662	4.0	placental lactogen 1	U2af2	X64587	-2.0	splicing factor
Adfp	M93275	2.9	adipose differentiation	Mor1	X07295	-2.5	malate dehydrogenase
Crya2	M73741	2.7	a-B2-crystallin gene	Scd2	M26270	-3.4	stearoyl-coA desaturase 2
Tcte3	M26332	2.2	T-complex testis gene	Jup	M90365	-4	plakoglobin
Ctla2a	X15591	-4.4	cytotoxic T lymphocyte	Gjb2	M81445	-21.4	connexin (Cx26) gene

We used four T-antigen-transformed lines and four Trp53-mutant cultures to synthesize targets for hybridization to oligonucleotide arrays. Comparisons were made between Dnmt11lox/1lox and Dnmt12lox/2lox cells (infected with pMXCP and pMXpuro, respectively) as both SV40-transformed and Trp53-mutant fibroblasts. Genes induced greater than twofold with a P value ≤ 0.05 (Student's paired t-test) are included in this list. The number of present calls out of the total 16 scans are indicated for each gene (No.). A subset of known genes that have been categorized based on function are shown. The complete list of genes and ESTs is available (<http://staffa.wi.mit.edu/jaenisch/ng2000>).



**Fig. 6** Gene induction in *Dnmt1*-mutant fibroblasts. Northern-blot analysis of mutant *Dnmt1*<sup>1lox/1lox</sup> and control *Dnmt1*<sup>2lox/2lox</sup> SV40-transformed cells at 6 to 12 days following Cre expression reveals high-level expression of both IAP elements and *Cdkn1c* in demethylated cells. *Dnmt1* and *GAPDH* are included as controls.

To attempt to correlate the cell-growth phenotype of *Dnmt1*-deficient cells with the expression profile, we noted the induction of the Cdk inhibitors *Cdkn1a* (encoding p21; Table 2) and *Cdkn1c* (encoding p57Kip2), which was identified in preliminary experiments using low-density arrays. Northern analysis confirmed the induction of *Cdkn1c* by demethylation (Fig. 6). Although there may be other genes that contribute to the inhibition of cell growth in these cultures, the induction of *Cdkn1a* and *Cdkn1c* may be among the changes in expression that cause *Dnmt1*-deficient cells to stop dividing.

#### RNA-FISH reveals variation between cells in demethylation-induced IAP activation

The importance of DNA methylation in silencing of endogenous retroviral elements has been well established. It has been suggested that expression of IAP elements leading to retrotransposition and rampant chromosome instability is one cause of lethality for *Dnmt1*-mutant embryos<sup>30</sup>. As seven IAP feature sets on the GeneCHIPs showed highly abundant IAP expression in *Dnmt1*-mutant cultures, yet one IAP feature set was downregulated (Table 2), we sought to address their role in the *Dnmt1*-mutant phenotype. To determine the range of IAP expression throughout demethylated fibroblast cultures, we used RNA-FISH to detect stable cytoplasmic transcripts that might identify active IAPs. We saw stochastic high-level expression in 39% of *Dnmt1*<sup>1lox/1lox</sup> cells (Fig. 7). The lack of detectable IAP expression in most cells indicates that mutagenesis caused by retrotransposition is not the major determinant that limits their lifespan, although we cannot exclude that IAP expression may contribute to p53-independent apoptosis.

#### Discussion

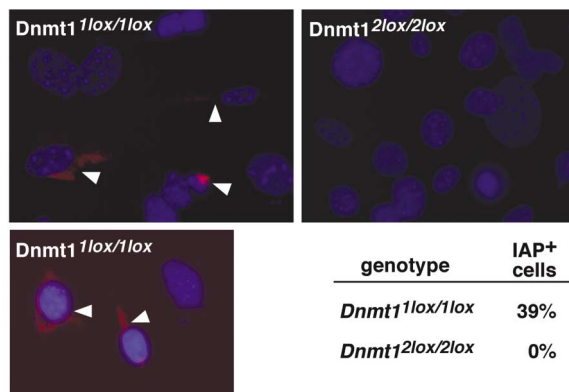
The essential role for DNA methylation in postgastrulation embryonic development led us to address the requirement for methylation in somatic cells. In contrast to embryonic cell types such as ES cells, which tolerate loss of *Dnmt1* despite widespread genomic demethylation<sup>4,5</sup>, *Dnmt1*-deficient primary mouse embryonic fibroblasts undergo a p53-dependent cell death

between five and six days after transduction with Cre (Fig. 3b). Considering the 24-hour cell cycle, and accounting for expression of Cre, inactivation of *Dnmt1* and turnover of *Dnmt1*, we estimate that these cells go through between two and four divisions before dying. Evidence from primary neuronal cultures and T-cell cultures are also consistent with this estimate<sup>31</sup> (P.L. and C.W., unpublished data). This rapid and uniform death is in contrast to the stochastic cell death observed in dying *Dnmt1*-mutant embryos and differentiating cultures of *Dnmt1*-mutant ES cells, which complicated previous mechanistic studies of demethylation-mediated cell death<sup>5,9</sup>. The onset of cell death occurred after deletion of *Dnmt1* when the genome was extensively if not completely demethylated (Fig. 2b), emphasizing a causal role of DNA methylation in cell survival. It is noteworthy that p53 is inactive in ES cells<sup>32</sup>, which may explain the viability of *Dnmt1*-deficient ES cells despite global demethylation. Thus, our data indicate that loss of DNA methylation in differentiated somatic cells provides a signal through p53, leading to apoptosis.

What are the signals that cause demethylated cells to die? We consider two non-exclusive alternatives: demethylation may activate the expression of genes that in turn activate p53, or demethylation may lead to the release of chromosomal proteins that serve as sensors for methylation status and cause p53 activation. For example, whereas p53 activation in primary fibroblasts usually leads to cell-cycle arrest in G1, demethylation could activate genes (such as *c-myc*; ref. 33) that cause cells to undergo apoptosis. Expression profiling of primary cells before apoptosis may identify candidate genes to test this model. *Traf3*, *Traf4* and *Adprp*, which were induced here, may also have roles in the apoptotic phenotype of the *Dnmt1*-mutant cultures. Several proteins can also be considered as possible mediators of the lethal *Dnmt1* phenotype, including methylation-dependent DNA binding proteins<sup>34</sup> and proteins that interact with *Dnmt1*, such as *Daxx* (ref. 35) and *Pcna* (ref. 27). In particular, the loss of *Dnmt1* from replication foci may block DNA replication in primary cells, in turn activating an apoptotic response through p53. It is also possible that demethylation causes DNA damage<sup>14</sup>, which indirectly leads to cell death. Dissecting how demethylation leads to p53-mediated cell death will be important for the understanding of how tumor cells acquire global demethylation. We have previously shown that *Dnmt1*-deficient ES cells have elevated rates of mitotic recombination and chromosome deletions<sup>14</sup>. Global demethylation and p53 mutational inactivation are both observed in a high percentage of human tumors<sup>12,20</sup>. Therefore, it is possible that loss of *Trp53* is required to select for tumor cells that tolerate demethylation, which in turn leads to genetic instability.

The ability of *Trp53* inactivation to rescue the *Dnmt1* lethal phenotype allowed us to characterize two additional phenotypes caused by demethylation and to correlate them with changes in mRNA expression by transcriptional profiling. First, a significant fraction of the *Dnmt1* *Trp53* double-mutant fibroblasts undergo p53-independent apoptosis (Fig. 3b). Several genes known to be involved in apoptotic response were deregulated in *Dnmt1*-mutant cells (Table 2), but we cannot determine which of these changes are direct effects of demethylation and which are indirect. Two methylation-dependent loci, IAP elements and *Xist*, were found to be overexpressed in *Dnmt1*-mutant fibroblasts. It is possible that the highly demethylation-inducible IAP transcripts (Table 2 and Fig. 6) may be one determinant of p53-independent apoptosis, consistent with the suggestion that DNA methylation is required to prevent deleterious effects of endogenous IAP activation<sup>30,36</sup>. The design of an inducible IAP element that is independent of DNA methylation status would serve to test the importance of IAP RNA expression to the cellular phenotype. Similarly, *Xist* expression has previously been shown to cor-

**Fig. 7** Cytoplasmic localization of IAP transcripts by RNA-FISH. A Cy3-labeled IAP probe (red) hybridized to mutant *Dnmt1*<sup>1lox/1lox</sup> and control *Dnmt1*<sup>2lox/2lox</sup> SV40-transformed cells shows high cytoplasmic expression in a subset of demethylated cells. We counted four mutant and three control cell lines to determine the percentage of IAP-positive cells. At least 300 cells were counted for each genotype.



relate with ectopic X inactivation and apoptosis in *Dnmt1*-mutant embryos<sup>9</sup>. The availability of a targeted *Xist* mutation<sup>37</sup> will allow a direct test of the importance of *Xist* activation in p53-independent apoptosis in *Dnmt1*-mutant cells.

The second notable phenotype of *Dnmt1 Trp53* double-mutant fibroblasts is a reduced rate of proliferation and a finite number of cell doublings (Fig. 3c). As *Dnmt1* is known to be an integral component of replication complexes, reduced proliferation may not be caused by epigenetic deregulation, but rather more directly through less stable association of replication factors in the absence of *Dnmt1*. Elevated expression of the cyclin-dependent kinase inhibitors p21 and p57 by demethylation (Table 2 and Fig. 6), however, may contribute to the slowed growth of these cells. Our data provide evidence for a direct role for *Dnmt1* in the control of cell proliferation. Both genetic and pharmacologic inhibition of *Dnmt1* have been shown to suppress tumor formation in mouse models<sup>13,38</sup>. Our data are consistent with either increased apoptosis or reduced cell proliferation as mechanisms by which inhibition of *Dnmt1* may prevent tumor initiation and development. The complete block to cell proliferation in the *Dnmt1 Trp53* double-mutant fibroblasts after five population doublings further supports the notion that *Dnmt1* may be an appropriate target for anti-cancer therapies.

Our findings contrast with recent results<sup>39</sup> that showed immortal cell growth was retained in a human colon cancer cell line following deletion of *DNMT1* by gene targeting. Because these *DNMT1*-mutant tumor cells showed only moderate genomic demethylation, it is possible, as the authors have suggested, that additional DNA methyltransferases can compensate for loss of *DNMT1*. This implies that the proliferation block we see in *Dnmt1 Trp53*-deficient primary mouse fibroblasts is either species-specific or is present in normal but not in tumor cells. A pharmacologic methyltransferase inhibitor, however, has been shown to block DNA replication in another human cancer cell line<sup>40</sup>. Alternatively, the targeted *DNMT1* allele may have not resulted in a null mutation, but rather a hypomorphic allele with low levels of methyltransferase activity sufficient for supporting cell proliferation. It will be important to test each of these possibilities to resolve these issues in the future.

Finally, we have analyzed approximately 10% of all mouse genes by transcription profiling to identify genes induced by demethylation. More than 600 genes, or nearly 10% of those expressed in the GeneCHIP assay, were shown to require DNA methylation for proper regulation among the p53-deficient fibroblast and the combined p53-deficient and T-antigen-transformed data sets (Table 2; <http://staffa.wi.mit.edu/jaenisch/ng2000>). Fewer genes were consistently deregulated among the transformed cell lines most likely due to changes in expression patterns known to occur in cell lines over time in culture. The consistency of the expression changes observed in the *Trp53*-deficient data set may be a result of the minimal time period used to generate the *Dnmt1 Trp53*-deficient and control fibroblast cultures (6 days). Analysis of the numbers of induced compared with repressed genes suggests that DNA hypomethylation causes global induction of gene expression. We offer this as a tentative conclusion, as we cannot at this point determine which are primary and which are secondary causes of demethylation. Nonetheless, biochemical analysis of *Dnmt1* protein complexes have revealed colocalization and direct interaction with histone

deacetylases<sup>41–43</sup>, which further supports the idea that *Dnmt1* mediates genome-wide transcriptional regulation perhaps directly as well as through changes in chromatin structure.

The role of methylation in gene expression in development has been subject to much speculation and debate<sup>44,45</sup>. It has been suggested that DNA methylation evolved solely as a defense mechanism against transposable elements and has no role in developmental gene repression<sup>30</sup>. Support for the defense hypothesis came from the analysis of *Dnmt1* hypomorphic mutant embryos which were shown to express high levels of IAP endogenous retroviral elements<sup>36</sup>, yet failed to show deregulation of several tissue-specific genes<sup>46</sup>. Due to stochastic cell death in *Dnmt1*-mutant embryos<sup>3,9</sup> and incomplete demethylation of individual genes before the mutant embryos die, however, it was difficult to draw a strong conclusion from these limited data. In contrast, in comparing homogeneous and extensively demethylated populations of differentiated cells, we found that DNA methylation is required to silence tissue-specific genes such as placental-specific *Pl1* (ref. 47) and germline-specific *Dazl* (ref. 48). Our results are also consistent with *Dnmt1* depletion experiments in *X. laevis* embryos, which showed premature transcriptional activation of several developmentally regulated genes<sup>10</sup>. These studies point to an essential function of DNA methylation in silencing gene expression during development<sup>29</sup>. Systematic tests of expression, methylation status and mutational inactivation for the demethylation-induced genes will be required to fully appreciate which of these genes are important determinants of the *Dnmt1*-mutant phenotype, and will address whether they are directly or indirectly controlled by loss of *Dnmt1*.

## Methods

**ES cells and mice.** We generated the targeting vector by subcloning a *loxP* site oligonucleotide into the *EcoRV* site of intron 3 in a plasmid with the 5-kb *BamHI* fragment containing exons 2–5. The selection cassette CMV-hygro-*tk* was subcloned into pBS246 to generate a floxed cassette which was inserted into the downstream *BamHI* site. The adjacent 3-kb *BamHI* fragment was inserted downstream of the selection cassette to create the 3' homology arm. The final vector, clone 18, was linearized with *NotI* and transfected by electroporation into J1 ES cells. Clones were selected with hygromycin (140 µg/ml; Calbiochem) and screened by Southern-blot analysis using an external 5' probe to identify targeted lines. We screened for the presence of the unselected 5' *loxP* site by PCR, and those clones were used for transient transfection with Cre to remove the CMV-hygro-*tk* cassette by counterselection with gancyclovir (2 µg/ml). A *Dnmt1*<sup>2lox/+</sup> cell line was used for a second round of targeting with clone 18 followed by Cre-mediated excision of both alleles to create the *Dnmt1*<sup>1lox/1lox</sup> cell line.

We injected two *Dnmt1*<sup>2lox/+</sup> cell lines into BALB/C host blastocysts to generate germline chimeras. These were crossed to wild-type 129SvJae mice to generate the inbred *Dnmt1*<sup>2lox/2lox</sup> strain used here. We also back-



# article

crossed the *Trp53*-mutant allele<sup>24</sup> to the 129SvJae substrain for more than six generations before establishing the *Trp53*<sup>-/-</sup>; *Dnmt1*<sup>2lox/2lox</sup> strain. The hypomorphic *Dnmt*<sup>n</sup> (ref. 5) allele and the *Dnmt*<sup>e</sup> (ref. 4) null allele have been described.

**Fibroblast isolation and genotyping.** Primary mouse embryo fibroblasts were isolated at 13.5 days post coitum by decapitation and evisceration of embryos. Individual carcasses were minced, trypsinized briefly, then disrupted by extensive pipeting. DNA was extracted from internal organs and used for PCR genotyping. Primers for the *Dnmt1* 5' lox site were *Dnmt1*-1 (5'-GGGCCAGTTGTGTGACTTGG-3') and *Dnmt1*-2 (5'-CTTGGCCCTGGATCTTGGGGA-3'), which amplify a 334-bp fragment from the wild-type allele and a 368-bp fragment from the *Dnmt1*<sup>2lox</sup> allele, respectively. Primers used to determine embryo sex amplify a 616-bp fragment from *Zfy1* and *Zfy2* (*ZfyE*, 5'-GATAAGCTTACATAATCATGGA-3', and *ZfyR*, 5'-CCTATGAAATCCTTTGCTGC-3'). Primers to genotype *Trp53* have been described<sup>24</sup>.

**Retroviral infections.** We carried out T-antigen–transformation by infection with supernatant from the producer cell line  $\phi$ 2-SV40 (ref. 49). pMX-CP was constructed by subcloning the *cre* ORF amplified by PCR from pOG231 (ref. 50) into pMX-puro (ref. 19). Cre retroviral supernatants were generated by transfecting the ecotropic packaging Phoenix cells with the pMXCP vector by the Calcium Phosphate method. We plated  $5 \times 10^5$  fibroblasts in wells of a 6-well dish and infected them with supernatant (1.5 ml) containing polybrene (4  $\mu$ g/ml; Sigma) by spinning at 2,400 r.p.m. for 45 min. Cells were passaged 12–24 h post-infection and selection with puromycin (4  $\mu$ g/ml) was started 24–36 h post-infection. Control experiments with pMXgfp (a gift from J. Bogan) showed that greater than 70% of cells were infected by this protocol.

**Southern blots.** DNA was isolated by cell lysis in Tris (0.1 M, pH 8.5), NaCl (0.2 M), EDTA (5 mM), 0.2% SDS, proteinase K (0.2 mg/ml) overnight at 50 °C, extraction with phenol-chloroform and isopropanol precipitation. Following restriction digestion DNAs were electrophoresed in 0.8% gels, acid nicked, denatured and transferred to Zetabind membranes with 10 $\times$ SSC. Hybridizations were carried out as described<sup>51</sup>.

**TUNEL assays.** Cells were permeabilized with 0.1% Triton for 2 min, fixed for 10 min in 4% paraformaldehyde in PBS, and stored in 70% ethanol before assay. Slides were equilibrated in terminal transferase buffer (Roche) and incubated for 60 min with TdT (200 U/ml) and biotin-16-dUTP (10  $\mu$ M; Roche). Following two washes with 4 $\times$ SSC TUNEL-positive cells were detected with avidin-Texas Red (1:100, Jackson).

**Oligonucleotide array analysis.** Targets were prepared from total RNA (20  $\mu$ g) as described<sup>28</sup>. We hybridized antisense target cRNA (10  $\mu$ g) to each array. Comparisons were made using four separate T-antigen–transformed lines (3 male and 1 female, all were between passages 3 and 7 following infection with the T antigen retrovirus) and four individual *Trp53*-mutant mEF cultures (2 male, 2 female; infected at passage 1) with and without Cre. Targets were hybridized to high-density arrays of 11,000 genes and ESTs (Murine11K GeneChIPs, Affymetrix), which were washed and amplified with a biotinylated anti-streptavidin antibody as recommended by the manufacturer before scanning.

**Statistical analysis.** We analyzed three data sets: (a) *Trp53*-deficient cells, including 4 independent scans each for *Dnmt1* mutant; (b) control T-antigen–transformed cell lines, including 4 independent scans each for *Dnmt1* mutant and controls; and (c) the combined (a) and (b) data sets. The primary scan data was analyzed using a Pearson correlation to determine which scan was most correlated to the rest of the data set. This was set as the reference scan. We used linear regression to determine the scaling factor for each scan relative to the reference scan. All data points below 50 were set to the threshold value of 50. Absent/present calls were used to eliminate spurious and non-expressed genes by requiring a minimum of 3 present calls out of 8 for both (a) and (b) data sets and 4 or more present calls for the combined (c) data set. *P* values were then calculated for all genes in the paired data sets comparing values from *Dnmt1* mutant with wild-type control cells using the Student's *t*-test (paired). Fold change was

calculated by averaging the values for mutant or wild-type and determining their ratio. Only genes with at least a twofold or higher change in expression and a *P* value of <0.05 are considered significant in this analysis.

**Hierarchical clustering.** Fold-change data for 1204 genes exhibiting a twofold or greater change in expression and a *P* value of <0.05 were clustered using established algorithms<sup>52</sup>. The data were analyzed by average linkage clustering using uncentered correlation of the log transformed fold-change data (demethylated average difference value/control average difference value) for the eight cell populations.

**Western-blot analysis.** An anti-*Dnmt1* antibody generated in chickens to a carboxy-terminal peptide from mouse *Dnmt1* has been described<sup>53</sup>. ES cells were lysed directly in Laemmli buffer and sonicated before electrophoresis. We confirmed western-blot transfer to Immobilon-ECL by PonceauS staining, and detected the *Dnmt1* antibody using an anti-chicken IgY-HRP conjugate (Promega) followed by ECL detection (Amersham).

**RNA-FISH.** Cells were permeabilized with 0.1% Triton for 2 min, fixed for 10 min in 4% paraformaldehyde in PBS, and stored in 70% ethanol before hybridization. The IAP probe was generated by incorporation of Cy3 labeled dCTP by PCR, and cells were visualized directly following hybridization and washing as described<sup>9</sup>.

**Supplementary information.** The microarray data set is available (<http://staffa.wi.mit.edu/jaenisch/ng2000>).

## Acknowledgments

We thank T. Golub for discussion regarding the Affymetrix GeneCHIP array experiments; M. Gaasenbeek, C. Heard, K. McClure and J. Park for training and technical assistance with GeneCHIP scanning; U. Pettersson for help with pilot experiments using adenovirus to transduce Cre into the *Dnmt1*<sup>2lox</sup> cultures; E. Koh and S. Cherry for advice on retroviral infections; B. Sauer for the loxP cassette pBS246; S. O'Gorman for the cre vector pOG231; J. Bogan for pMXpuro and pMXgfp; E. Koh for Phoenix cells; A. Fazeli and R. Weinberg for the *p53* mutant mice; and T. Bestor for the IAP probe. L.J.G. was supported by the NIH and Pfizer. Funding for this work was through NIH grants R-35-CA44339 (R.J.) and HD18184 (C.W.), the March of Dimes (C.W.), and grants from Affymetrix Inc., Millenium Pharmaceuticals Inc., and Bristol-Meyers Squibb Company.

Received 11 April; accepted 4 October 2000.

- Wolffe, A.P. & Matzke, M.A. Epigenetics: regulation through repression. *Science* **286**, 481–486 (1999).
- Bird, A.P. & Wolffe, A.P. Methylation-induced repression—belts, braces, and chromatin. *Cell* **99**, 451–454 (1999).
- Jaenisch, R. DNA methylation and imprinting: why bother? *Trends Genet.* **13**, 323–329 (1997).
- Lei, H. *et al.* De novo DNA cytosine methyltransferase activities in mouse embryonic stem cells. *Development* **122**, 3195–3205 (1996).
- Li, E., Bestor, T.H. & Jaenisch, R. Targeted mutation of the DNA methyltransferase gene results in embryonic lethality. *Cell* **69**, 915–926 (1992).
- Okano, M., Bell, D.W., Haber, D.A. & Li, E. DNA methyltransferases *Dnmt3a* and *Dnmt3b* are essential for de novo methylation and mammalian development. *Cell* **99**, 247–257 (1999).
- Li, E., Beard, C. & Jaenisch, R. Role for DNA methylation in genomic imprinting. *Nature* **366**, 362–365 (1993).
- Beard, C., Li, E. & Jaenisch, R. Loss of methylation activates *Xist* in somatic but not in embryonic cells. *Genes Dev.* **9**, 2325–2334 (1995).
- Panning, B. & Jaenisch, R. DNA hypomethylation can activate *Xist* expression and silence X-linked genes. *Genes Dev.* **10**, 1991–2002 (1996).
- Stancheva, I. & Meehan, R.R. Transient depletion of *xDnmt1* leads to premature gene activation in *Xenopus* embryos. *Genes Dev.* **14**, 313–327 (2000).
- Bayliss, S.B. & Herman, J.G. DNA hypermethylation in tumorigenesis: epigenetics joins genetics. *Trends Genet.* **16**, 168–174 (2000).
- Jones, P.A. & Laird, P.W. Cancer epigenetics comes of age. *Nature Genet.* **21**, 163–167 (1999).
- Laird, P.W. *et al.* Suppression of intestinal neoplasia by DNA hypomethylation. *Cell* **81**, 197–205 (1995).
- Chen, R.Z., Pettersson, U., Beard, C., Jackson-Grusby, L. & Jaenisch, R. DNA hypomethylation leads to elevated mutation rates. *Nature* **395**, 89–93 (1998).
- Hansen, R.S. *et al.* The DNMT3B DNA methyltransferase gene is mutated in the ICF immunodeficiency syndrome. *Proc. Natl. Acad. Sci. USA* **96**, 14412–14417 (1999).
- Xu, G.L. *et al.* Chromosome instability and immunodeficiency syndrome caused by mutations in a DNA methyltransferase gene. *Nature* **402**, 187–191 (1999).
- Sauer, B. & Henderson, N. Site-specific DNA recombination in mammalian cells by the Cre recombinase of bacteriophage P1. *Proc. Natl. Acad. Sci. USA* **85**, 5166–5170 (1988).



18. Margot, J.B. *et al.* Structure and function of the mouse DNA methyltransferase gene: Dnmt1 shows a tripartite structure. *J. Mol. Biol.* **297**, 293–300 (2000).
19. Onishi, M. *et al.* Applications of retrovirus-mediated expression cloning. *Exp. Hematol.* **24**, 324–329 (1996).
20. Levine, A.J. p53, the cellular gatekeeper for growth and division. *Cell* **88**, 323–331 (1997).
21. Hakem, R., de la Pompa, J.L., Elia, A., Potter, J. & Mak, T.W. Partial rescue of Brca1 (5-6) early embryonic lethality by p53 or p21 null mutation. *Nature Genet.* **16**, 298–302 (1997).
22. Lim, D.S. & Hasty, P. A mutation in mouse rad51 results in an early embryonic lethal that is suppressed by a mutation in p53. *Mol. Cell. Biol.* **16**, 7133–7143 (1996).
23. Ludwig, T., Chapman, D.L., Papaioannou, V.E. & Efstratiadis, A. Targeted mutations of breast cancer susceptibility gene homologs in mice: lethal phenotypes of Brca1, Brca2, Brca1/Brca2, Brca1/p53, and Brca2/p53 nullizygous embryos. *Genes Dev.* **11**, 1226–1241 (1997).
24. Jacks, T. *et al.* Tumor spectrum analysis in p53-mutant mice. *Curr. Biol.* **4**, 1–7 (1994).
25. Emerman, M. & Temin, H.M. Genes with promoters in retrovirus vectors can be independently suppressed by an epigenetic mechanism. *Cell* **39**, 449–467 (1984).
26. Leonhardt, H., Page, A.W., Weier, H.U. & Bestor, T.H. A targeting sequence directs DNA methyltransferase to sites of DNA replication in mammalian nuclei. *Cell* **71**, 865–873 (1992).
27. Chuang, L.S. *et al.* Human DNA-(cytosine-5) methyltransferase-PCNA complex as a target for p21WAF1. *Science* **277**, 1996–2000 (1997).
28. Fambrough, D., McClure, K., Kazlauskas, A. & Lander, E.S. Diverse signaling pathways activated by growth factor receptors induce broadly overlapping, rather than independent, sets of genes. *Cell* **97**, 727–741 (1999).
29. Bird, A. & Tweedie, S. Transcriptional noise and the evolution of gene number. *Philos. Trans. R. Soc. Lond. B. Biol. Sci.* **349**, 249–253 (1995).
30. Yoder, J.A., Walsh, C.P. & Bestor, T.H. Cytosine methylation and the ecology of intragenomic parasites. *Trends Genet.* **13**, 335–340 (1997).
31. Fan, G.P. *et al.* DNA hypomethylation perturbs the function and survival of CNS neurons in postnatal animals. *J. Neurosci.* (in press).
32. Sabapathy, K., Klemm, M., Jaenisch, R. & Wagner, E.F. Regulation of ES cell differentiation by functional and conformational modulation of p53. *EMBO J.* **16**, 6217–6229 (1997).
33. Hermeking, H. & Eick, D. Mediation of c-Myc-induced apoptosis by p53. *Science* **265**, 2091–2093 (1994).
34. Hendrich, B. & Bird, A. Identification and characterization of a family of mammalian methyl-CpG binding proteins. *Mol. Cell. Biol.* **18**, 6538–6547 (1998).
35. Michaelson, J.S., Bader, D., Kuo, F., Kozak, C. & Leder, P. Loss of Daxx, a promiscuously interacting protein, results in extensive apoptosis in early mouse development. *Genes Dev.* **13**, 1918–1923 (1999).
36. Walsh, C.P., Chaillet, J.R. & Bestor, T.H. Transcription of IAP endogenous retroviruses is constrained by cytosine methylation. *Nature Genet.* **20**, 116–117 (1998).
37. Marahrens, Y., Panning, B., Dausman, J., Strauss, W. & Jaenisch, R. Xist-deficient mice are defective in dosage compensation but not spermatogenesis. *Genes Dev.* **11**, 156–166 (1997).
38. Cormier, R.T. & Dove, W.F. Dnmt1N/+ reduces the net growth rate and multiplicity of intestinal adenomas in C57BL/6-multiple intestinal neoplasia (Min)/+ mice independently of p53 but demonstrates strong synergy with the modifier of Min 1(AKR) resistance allele. *Cancer Res.* **60**, 3965–3970 (2000).
39. Rhee, I. *et al.* CpG methylation is maintained in human cancer cells lacking DNMT1. *Nature* **404**, 1003–1007 (2000).
40. Knox, J.D. *et al.* Inhibition of DNA methyltransferase inhibits DNA replication. *J. Biol. Chem.* **275**, 17986–17990 (2000).
41. Fuks, F., Burgers, W.A., Brehm, A., Hughes-Davies, L. & Kouzarides, T. DNA methyltransferase Dnmt1 associates with histone deacetylase activity. *Nature Genet.* **24**, 88–91 (2000).
42. Robertson, K.D. *et al.* DNMT1 forms a complex with rb, E2F1 and HDAC1 and represses transcription from E2F-responsive promoters. *Nature Genet.* **25**, 338–342 (2000).
43. Rountree, M.R., Bachman, K.E. & Baylin, S.B. DNMT1 binds HDAC2 and a new co-repressor, DMAP1, to form a complex at replication foci. *Nature Genet.* **25**, 269–277 (2000).
44. Bird, A. Does DNA methylation control transposition of selfish elements in the germline? *Trends Genet.* **13**, p469–472 (1997).
45. Yoder, J.A., Walsh, C.P. & Bestor, T.H. Cytosine methylation and the ecology of intragenomic parasites. *Trends Genet.* **13**, 335–340 (1997).
46. Walsh, C.P. & Bestor, T.H. Cytosine methylation and mammalian development. *Genes Dev.* **13**, 26–34 (1999).
47. Colosi, P., Talamantes, F. & Linzer, D.I. Molecular cloning and expression of mouse placental lactogen I complementary deoxyribonucleic acid. *Mol. Endocrinol.* **1**, 767–776 (1987).
48. Ruggiu, M. *et al.* The mouse *Dazl* gene encodes a cytoplasmic protein essential for gametogenesis. *Nature* **389**, 73–77 (1997).
49. Jat, P.S., Cepko, C.L., Mulligan, R.C. & Sharp, P.A. Recombinant retroviruses encoding simian virus 40 large T antigen and polyomavirus large and middle T antigens. *Mol. Cell. Biol.* **6**, 1204–1217 (1986).
50. O’Gorman, S., Dagenais, N.A., Qian, M. & Marchuk, Y. Protamine-Cre recombinase transgenes efficiently recombine target sequences in the male germ line of mice, but not in embryonic stem cells. *Proc. Natl. Acad. Sci. USA* **94**, 14602–14607 (1997).
51. Church, G.M. & Gilbert, W. Genomic sequencing. *Proc. Natl. Acad. Sci. USA* **81**, 1991–1995 (1984).
52. Eisen, M.B., Spellman, P.T., Brown, P.O. & Botstein, D. Cluster analysis and display of genome-wide expression patterns. *Proc. Natl. Acad. Sci. USA* **95**, 14863–14868 (1998).
53. Gaudet, F., Talbot, D., Leonhardt, H. & Jaenisch, R. A short DNA methyltransferase isoform restores methylation in vivo. *J. Biol. Chem.* **273**, 32725–32729 (1998).